Received: July 25, 2022. Revised: August 27, 2022.

INASS

International Journal of
Intelligent Engineering & Systems

http://www.inass.org/

Oscillation Damping Emulation Using Superconducting Magnetic Energy Storage based on Sine Cosine Algorithm on Jawa Indonesian Power Grid

Muhammad Abdillah[1] Herlambang Setiadi[2]* IBG Manuaba[3] Imam Wahyudi Farid[4]
Agileswari K. Ramasamy[5] Renuga Verayiah[5] Maryati Binti Marsadek[6]

[1]Department of Electrical Engineering, Universitas Pertamina, Jakarta, Indonesia
[2]Faculty of Advanced Technology and Multidiscipline, Universitas Airlangga, Surabaya, Indonesia
[3]Department of Electrical Engineering, Universitas Udayana, Indonesia
[4]Automation Electronic Engineering, Faculty of Vocational Studies,
Institut Teknologi Sepuluh Nopember, Surabaya, Indonesia
[5]Department of Electrical and Electronics Engineering, Universiti Tenaga Nasional, Kajang, Malaysia
[6]Institute of Power Engineering, Universiti Tenaga Nasional, Kajang, Malaysia
*Corresponding author: h.setiadi@ftmm.unair.ac.id

Abstract: This paper proposed method for emulated oscillation damping using superconducting magnetic energy storage (SMES) devices. To find the best oscillation damping emulation the parameter of SMES is optimized using sine cosine algorithm (SCA). Jawa Indonesia power grid is used as the test system to observe the efficacy of the proposed controller method. Time domain simulation is carried out to investigate how the proposed method can be used to emulate the oscillation damping in the system. From the simulation results, it is noticeable that SMES based on SCA could be used to emulate the oscillation damping on the Jawa Indonesian power grid. This is indicated by the small overshoot and fast settling time of rotor speed dynamics response (Overshoot and settling time of Suralaya power plant -0.000448 and 5.51 second).

Keywords: Clean energy technology, Dynamics response, SCA, SMES.

1. Introduction

Dynamics stability of power system is the ability of power system to maintain the synchronization after being subjected by sHmall perturbation [1]. Generally, dynamics stability of power system can be handled by using damper windings in the rotor of the generator. However, over the time the performance of the generator can be compromised [2]. Alternately, the dynamic stability can be achieved when there is a balance between mechanical power and electrical power of the power system. This balance is usually done by controlling the governor of the generator to adjust the speed of the turbine when disturbance emerges. However, the response time of governor is much slower [3]. Hence, it is essential to have additional devices that could provide and store electrical energy in short amount of time.

Energy storage is one of the devices that can store and release electrical power in the short amount of time. There are various types of energy storage that has been used in research and industrial sector. Research effort in [4], proposed a method for reducing the rate of frequency change of by using capacitor energy storage. It is noticeable that the capacitor energy storage can reduced the overshoot of frequency as well as accelerate the frequency response to find the initial conditions. The application of capacitor energy storage as virtual inertia emulation is proposed in [5]. In [5], tidal power plant is used as the test system for investigate the performance of capacitor energy storage as virtual inertia control. From the findings, it was observed that the rate of frequency change (RoCof) can be reduced significantly by adding capacitor energy storage.

Researchers in [6] proposed a method to enhance

the small signal stability performance of power system using battery energy storage systems. The outcome of the adding battery energy storage system is increasing damping performance of electromechanical modes. In [7] the application of battery energy storage system for frequency stabilization was achieved with the right sizing and placement of the battery energy storage system.

The application of redox flow batteries as load frequency control of power system is reported in [8]. It is observed that by adding redox flow batteries on the power system can help the load frequency control to stabilize the frequency as well as maintaining balance between load and generating. The application of redox flow batteries as inertia support is reported in [9]. From the simulation results, it is observed that, redox flow can emulate inertia to the system in presence of inertia-less wind power plant. Among numerous types of energy storage above, superconducting magnetic energy storage (SMES) is getting more attraction currently [10].

The application of SMES for enhancing the power flow of power system is reported in [10]. In [10], microgrid system is used as the test system for testing the SMES performance. Wind power plant is also considered to simulate the effect of uncertainty power plant. From the simulation results it is observed that, SMES can optimally increase the power flow of the microgrid in the presence of intermittent wind power plant. Ansari M et all proposed application of SMES for enhancing frequency performance of power system as reported in [11]. Isolated wind-diesel hybrid power system is used as the test system in [11]. However, very scant attention has been made on the applications of SMES as power oscillation emulation. In addition, the design of SMES parameter is also essential. Hence, it is important to investigate the application of SMES as power oscillation emulation and how to optimally find the parameter of SMES.

Generally, for optimization problems, metaheuristic algorithms are one of the popular methods. Metaheuristic algorithms are not only helping engineers for reducing complexity using traditional mathematical approaches, but they also give optimal solutions from complex engineering problems. The application of particle swarm optimization and genetic algorithm for tuning Power System Stabilizer is reported in [12]. It is found that the complex parameter of PSS can be tuned without jeopardizing the stability performance of the systems. Research effort in [13], proposed application of firefly algorithms (FA) for designing excitation system controller. The purpose of the research is to find better controller value of excitation system controller. When the excitation system controller has optimal value, they can produce magnetic field on the synchronous generator optimally. It is noticeable from the results that FA can provide optimal value for the excitation controller compared to the other method. This is indicated by the stability of the power system that can be enhanced when excitation controller is tuned using FA. Shakarami et all proposed a novel method for designing wide-area power system stabilizer based on the grey wolf optimization (GWO) as reported in [14]. It is observed that the wide-area PSS based on GWO provide promising results for enhancing small signal stability of power systems. Optimal tuning of PSS based on bat algorithm (BA) is reported in [15]. It is found that BA can be used to tuned PSS parameter even in the uncertainty conditions due to integration of inverter-based power plant. A recent novel algorithm inspired by sine and cosine function for optimization problem called sine cosine algorithm (SCA) is developed. It is reported that SCA showing better performance in terms of convergence speed, optimal solution search precision and stability compared to approaches like in [16, 17].

This novelty is to use the advantages of the SCA such as the low number of parameters and lack of optimal local trapping to optimized parameters of SMES. By designing SMES using SCA the oscillation of Jawa Indonesia power grid can be damp significantly. The rest of the paper is organized as follows: section 2 focuses on dynamic modelling of power system and SMES. The optimization method is presented in section 3. In addition, section 4 shows the results and discussion of the research. Furthermore, the conclusions and future study of this paper is presented in section 5.

2. Modelling

2.1 Dynamic model of synchronous generator

In order to produce electrical energy a generator requires two inputs, the first is the turbine mechanical torque (T_m) and the second one is the magnetic field flux (E_{FD}). The mechanical torque is used to rotate the rotor of the generator. The magnetic field flux is generated from the field circuit through the windings contained in the rotor. In the presence of mechanical torque, the generator rotor rotates with a kinetic energy of $J\omega/2$ Joules. The representation of angular momentum can be described using Eq. (1) [18].

$$M = J\,\omega \tag{1}$$

With ω is rotor speed and J is the inertia moment. The flux generated by the rotor field coil with the current If will rotate and induce an electromotive

force on the stator coil of. The process of the electromotive force can be described using Eq. (2).

$$E = c\, n\, \varphi \tag{2}$$

If the synchronous generator is loaded, the generator current will flow to the load. This current produces a flux in the stator and will create an electric torque (T_e) against the mechanical torque. At steady state, the sum of the mechanical torque with the electric torque is equal to zero (T_m-T_e=0), and the generator will rotate at synchronous angular speed (ω_0). Before reaching steady state there is a transient period and this amount of torque causes acceleration torque and will result in acceleration or deceleration. The mathematical representation of motion in this condition can be described in Eq. (3) [19].

$$T_a = T_m - T_e = J\frac{d^2\delta_m}{dt^2} \tag{3}$$

Eq. (3) is multiplied by the angular velocity (ω_m), to get new mathematical expressions as described in (4). Eq. (4) can be further described using Eqs. (5) and (6) [20].

$$\omega_m J\frac{d^2\delta_m}{dt^2} = P_m - P_e = P_a \tag{4}$$

$$\frac{2}{\omega_m}\left(\frac{1}{2}{\omega_m}^2 J\right)\frac{d^2\delta_m}{dt^2} = P_m - P_e \tag{5}$$

$$\frac{2}{\omega_m}\frac{\left(\frac{1}{2}{\omega_m}^2 J\right)}{S}\frac{d^2\delta_m}{dt^2} = P_m - P_e \tag{6}$$

The mathematical representation of the total inertia produced by generator can be represented as Eq. (7).

$$H = \left(\frac{1}{2}{\omega_m}^2 J\right) \tag{7}$$

Hence, Eq. (7) can be further written as described in Eqs. (8), (9) and (10).

$$\frac{2H}{\omega_m}\frac{d^2\delta_m}{dt^2} = P_m - P_e \tag{8}$$

$$\omega_m = \frac{2}{p}\omega_s \tag{9}$$

$$\delta_m = \frac{2}{p}\delta \tag{10}$$

Eq. (8) is called the machine swing equation which is the basic equation governing the dynamics (motion) of synchronous machine rotation in stability studies. From these equations the difference between the mechanical power of the turbine and the electrical power of the generator causes the rotor angle to accelerate or decelerate. Since the engine has a torque component that is proportional to the angular velocity, the complete equation of rotor motion is expressed as Eq. (11) [21].

$$\frac{Md^2\delta_m}{\omega_0 dt^2} + \frac{Dd\delta_m}{\omega_0 dt} = T_m - T_e \tag{11}$$

Where D is the machine damping coefficient. A generator operating at steady state have the value of T_m equal to T_e. Furthermore, a small load is added which causes an increase in the stator field flux and a change in E'_q. Small changes also cause changes in machine angle and changes in electric torque. In addition, the electric torque will increase with increasing machine angle and stator flux. This process can be captured through Eq (12) [21].

$$\Delta T_e = \left(\frac{dT_e}{d\delta}\right)\Delta\delta + \left(\frac{dT_e}{dE'_q}\right)\Delta E'_q = K_1\Delta\delta + K_2\Delta E'_q \tag{12}$$

With,

$$K_1 = E_{q0}V_0\left(\frac{r_e\, sin(\delta_0-\alpha)+(X_e+X'_d)\, cos(\delta_0-\alpha)}{{r_e}^2+(X_e+X'_d)+(X_q+X_e)}\right) + I_{q0}\left(\frac{(X_e+X'_d)(X_q+X_e)\, sin(\delta_0-\alpha)-r_e(X_e-X'_d)\, cos(\delta_0-\alpha)}{{r_e}^2+(X_e+X'_d)+(X_q+X_e)}\right) \tag{13}$$

$$K_2 = \left(\frac{r_e E_{q0}}{{r_e}^2+(X_e+X'_d)+(X_q+X_e)}\right) + i_{q0}\left(\frac{(X_q+X_e)(X_q-X'_d)}{{r_e}^2+(X_e+X'_d)+(X_q+X_e)}\right) \tag{14}$$

If the mechanical torque is constant, then the rotor rotation equation for small load changes around the operating condition can be described using Eq. (15). In addition, the Eq. (15) can be transformed into laplace equations as described in Eq. (16) [21].

$$\frac{Md^2\delta_m}{\omega_0 dt^2} + \frac{Dd\delta_m}{\omega_0 dt} = -\Delta T_e \tag{15}$$

$$\frac{M}{\omega_0}S^2\Delta\delta + \frac{D}{\omega_0}S\Delta\delta = -\Delta T_e \tag{16}$$

The effect of a small load changes is also felt by the armature winding so that the field E'_q changes by $\Delta E'_q$, the magnitude of the change in field voltage is influenced by changes in the machine angle ($\Delta\delta$) and if the excitation field voltage is constant (ΔE_{FD}=0), then the mathematical representation of this phenomena can be described using Eq. (17) [21].

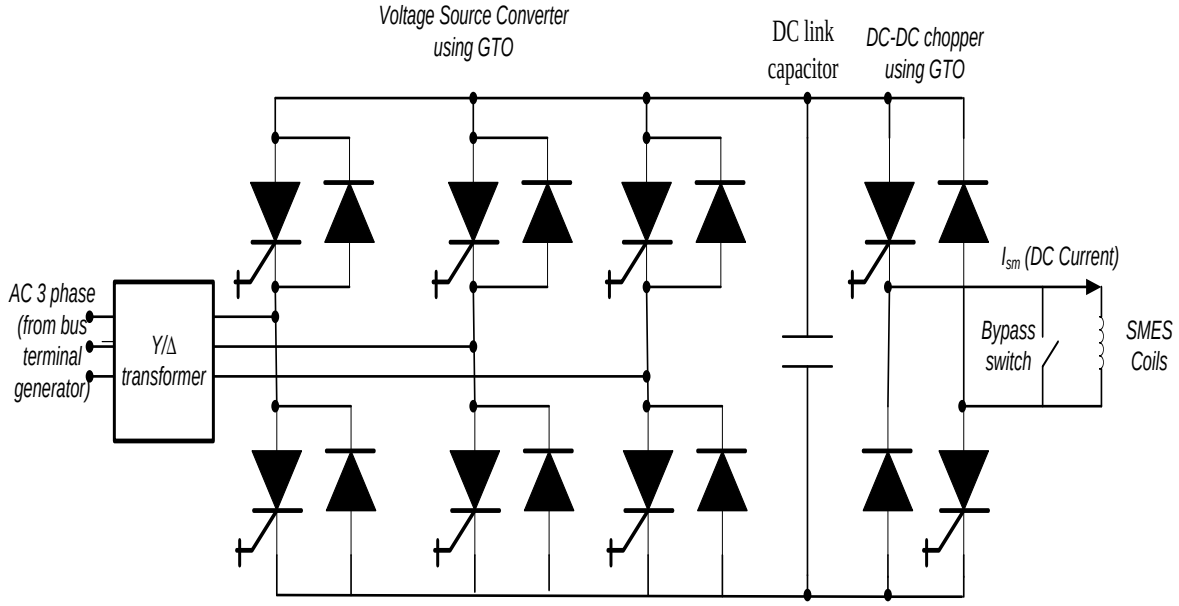

Figure. 1 SMES electrical circuits

$$\Delta E'_q = -\frac{K_3.K_4.\Delta\delta}{(1+sT_{d0}.K_3)} \quad (17)$$

With

$$K_3 = \left(1 + \frac{(X_e+X'_d)(X_q-X'_d)}{r_e{}^2+(X_e+X'_d)+(X_q+X_e)}\right)^{-1} \quad (18)$$

$$K_4 = \left(\frac{V_0(X_e+X'_d)\{(X_q+X_e)\,sin(\delta_0-\alpha)-r_e\,cos(\delta_0-\alpha)\}}{r_e{}^2+(X_e+X'_d)+(X_q+X_e)}\right)^{-1} \quad (19)$$

Furthermore, changes in field voltage affect the generator terminal voltage as well as changes in machine angle. The change in terminal voltage due to the changes in machine angle and changes in field voltage can be expressed using Eq. (20) [21].

$$\Delta V_t = K_5\Delta\delta + K_6\Delta E'_q \quad (20)$$

With

$$K_5 = \frac{V_D}{V_t}X_q\left(\frac{r_eV_0\,sin(\delta_0-\alpha)+(X_e+X'_d)\,cos(\delta_0-\alpha)}{r_e{}^2+(X_e+X'_d)+(X_q+X_e)}\right) + \frac{V_D}{V_t}X_d\left(\frac{r_eV_0\,cos(\delta_0-\alpha)-V_0(X_q+X_e)\,sin(\delta_0-\alpha)}{r_e{}^2+(X_e+X'_d)+(X_q+X_e)}\right) \quad (21)$$

$$K_6 = \frac{V_D}{V_t}\left(1 - \frac{X'_d(X_q+X_e)}{r_e{}^2+(X_e+X'_d)+(X_q+X_e)}\right) + \frac{V_D}{V_t}X_d\left(\frac{r_e}{r_e{}^2+(X_e+X'_d)+(X_q+X_e)}\right) \quad (22)$$

2.2 Dynamic model automatic voltage regulator

The automatic voltage regulator (AVR) is used to regulate the excitation field voltage (E_{FD}), the difference between the generator terminal voltage output and the desired voltage is the input for the AVR to regulate the excitation field voltage. If the change in the excitation field must be taken into account ($E_{FD} \neq 0$), then the dynamic behaviour can be captured using Eqs. (23) and (24).

$$\Delta E'_q = \frac{-K_3(\Delta E'_q-K_4)}{1+sT'_{d0}K_3} \quad (23)$$

With

$$\Delta E'_q = \frac{K_A}{1+sT_A}\Delta V_t \quad (24)$$

2.3 Dynamic model of turbine and governor

Water turbines and steam turbines are used in the Jawa 500 kV multi-machine system. The water turbine receives mechanical power from the thrust of water coming out of the dam's water pipe (penstock). Furthermore, this turbine produces mechanical power (torque), which is used to turn the generator. The turbine also has an auxiliary controller to control the rotation of the turbine. This controller is known as the governor. The linear model of the water turbine and governor can be easily formed in a linear mathematical representation Eqs. (25) and (26) [22].

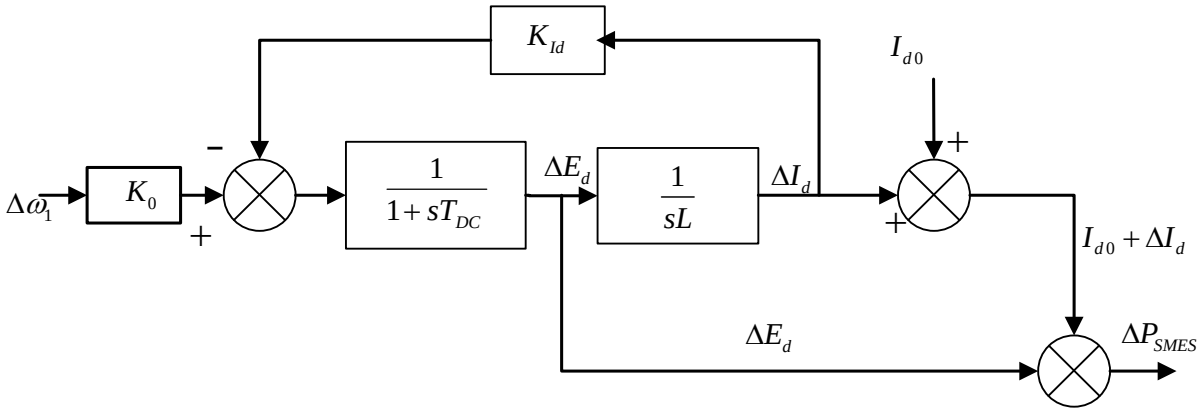

Figure. 2 SMES block diagram

$$\Delta\dot{T}_{Mi} = \left(\frac{2}{T_{wi}} + \frac{2}{T_{gwi}}\right)\Delta Y_i - \frac{2K_{gwi}\Delta U_{1i}}{T_{gwi}} + \frac{2K_{gwi}\Delta\omega_i}{R_i T_{gwi}} - \frac{2\Delta T_{mi}}{T_{wi}} \quad (25)$$

$$\Delta\dot{Y}_i = \frac{K_{gwi}}{T_{gwi}}\Delta U_{1i} + \frac{K_{gwi}\Delta\omega_i}{R_i T_{gwi}} - \frac{\Delta Y_i}{T_{gwi}} \quad (26)$$

The steam turbine receives mechanical energy from the steam boiler and produces mechanical energy (torque) to power the steam turbine. Eq. (27) and show the linear representation of the steam turbine model Eq. (28). The difference between a water turbine and a steam turbine in linear models is found in their parameter values. [22].

$$\Delta\dot{T}_{Mi} = \left(\frac{2}{T_{ui}} + \frac{2}{T_{gui}}\right)\Delta Y_i - \frac{2K_{gui}\Delta U_{1i}}{T_{gui}} + \frac{2K_{gui}\Delta\omega_i}{R_i T_{gui}} - \frac{2\Delta T_{mi}}{T_{ui}} \quad (27)$$

$$\Delta\dot{Y}_i = \frac{K_{gui}}{T_{gui}}\Delta U_{1i} - \frac{K_{gu}\Delta\omega_i}{T_{gui}R_i} - \frac{\Delta Y_i}{T_{gui}} \quad (28)$$

2.4 Superconducting magnetic energy storage

SMES in an electric power system is used to control the balance of power in the synchronous generator during the disturbance periods. SMES are installed in terminal bus generators on the power system model. Fig. 1 depicts the basic SMES configuration, which includes a Y- transformer, a voltage source converter using a GTO thyristor, a two quadrant DC-DC chopper using a GTO, and a superconducting coil. DC link capacitors connect the DC-DC converters and chopper.

In this paper the dynamic characteristics of SMES is essential. The dynamic characteristic of SMES can be captured through laplace representation as described in Eqs. (29) and (30). Fig. 2 shows the dynamic model of SMES.

$$\Delta E_d = \frac{1}{1+T_{dc}s}[k_0\Delta\omega_1 - k_{Id}\Delta I_d] \quad (29)$$

$$\Delta I_d = \frac{1}{Ls}\Delta E_d \quad (30)$$

Where k_{Id} is the gain for feedback *Id*, T_{dc} is the converter time delay, k_0 is the gain constant, and *L* is the coil inductance. The deviation in the SMES unit's inductor real power is expressed in time domain as described in Eq. (31). In addition, the energy stored in SMES can be mathematically described in Eq. (32).

$$\Delta P_{smes}(t) = \Delta I_{d0}\Delta E_d + \Delta I_d\Delta E_d \quad (31)$$

$$W_{smes}(t) = \frac{LI_d^2}{2} \quad (32)$$

3. Method

3.1 Test systems

Fig. 3 depicts a 500 kV Java Indonesia power grid, which serves as the third test system in this thesis. This system is divided into three areas that are linked by a high voltage transmission line that runs from the east side of Java island to the west side of Java island. The distance between areas 1 and 2 is 500 kilometres, and the distance between areas 2 and 3 is 500 kilometres. This system is made up of eight generator buses and seventeen bus loads. This system has a total generating capacity of 12417.8 MW. Furthermore, the system's total load is 10361 MW. [23].

3.2 Sine cosine algorithm

Sine cosine algorithm (SCA) is an optimization method based on a stochastic population that uses a mathematical model of the *sin* and *cos* functions that can solve multi-dimensional problems. The process will be conducted in several iteration stages. The

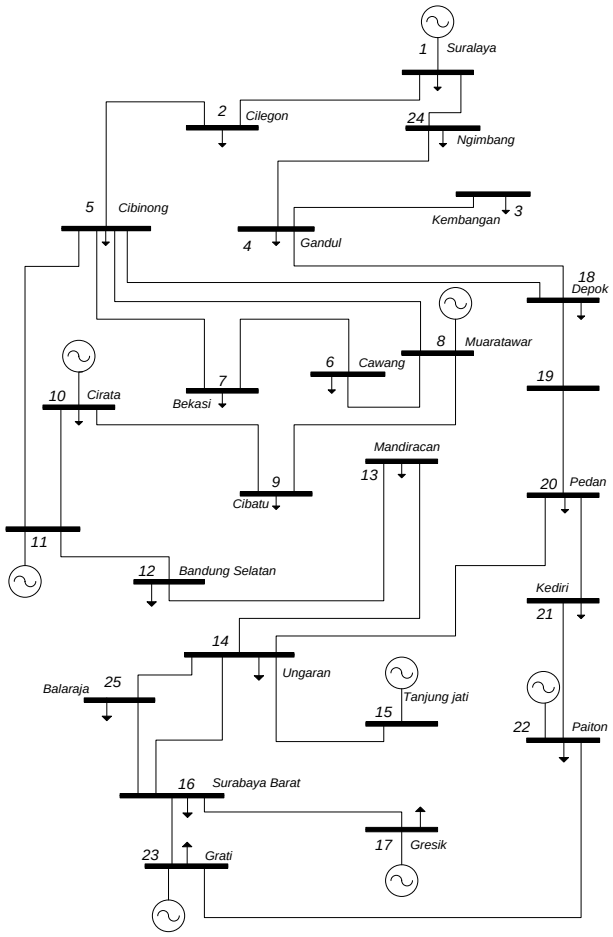

Figure. 3 Jawa Indonesia power grid single line diagram

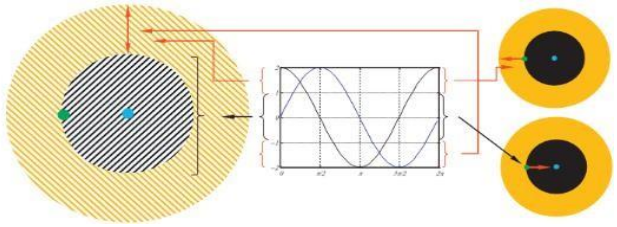

Figure. 4 Representation of SCA

iteration stage will only stop if the system has reached the maximum iteration value and finds the optimum solution value [24].

In the process of finding the best solution candidate value in each iteration, it is done using the equations sin and cos. The following are the equations used in the SCA algorithm.

$$X_i^{t+1} = \begin{cases} X_i^t + r_1 \times \sin(r_2) \times \left| r_3 p_i^t - x_i^t \right|, & r_4 < 0.5 \\ X_i^t + r_1 \times \cos(r_2) \times \left| r_3 p_i^t - x_i^t \right|, & r_4 \geq 0.5 \end{cases} \quad (33)$$

In the SCA method, the possibility of finding the optimum value occurs in the exploration phase. Afterward, in the exploitation phase, the algorithm will gradually reduce the value of the candidate solution until the optimum solution value is found [25]. The value of the parameter r_1 will decrease non-linearly. This happens because, in this paper, the optimization problem is included in the non-linear optimization type. In the exploration phase, the possibility of memory to store the search results is more and able to reduce the possibility of optima local solution results [26]. The following is the equation for the parameter value r_1 in the SCA method.

$$r_1 = a \times sin\left(\left(1 - \frac{t}{T}\right) \times \frac{\pi}{2}\right) + b \quad (34)$$

To represent SCA, the following image can be used.

3.3 Procedure of designing the controller

In this paper, SCA is used to design the parameter of SMES. SMES is added in same bus of Suralaya power plant. The procedure for designing SMES parameter using SCA include the following process:

a. Obtaining the required power system data (static and dynamic data)
b. Conduct the load flow of the power system to get the static data.
c. Linearize the non-linear system based of the load flow results conducted in section 1.
d. Initializing SCA parameter (maximum number of iterations, candidate solutions).
e. Evaluating each candidate and find temporary solution based on Eq. (35) value.

$$Minimum\ error = \int_0^t t|\Delta\omega(t)|dt \quad (35)$$

f. Updating the value of r_1 to determine the direction of movement of the best (temporary) solution candidate and also the values of 2, 3, and 4 because they are still related to the position of the candidate solution.
g. Fixing the position of the solution candidate.
h. The algorithm will stop iterating when it reaches the maximum number of iterations that have been determined.

The simulation is conducted in MATLAB for the SCA and SIMULINK for the power system and SMES. Fig. 5 shows the convergence graph of SMES based on SCA.

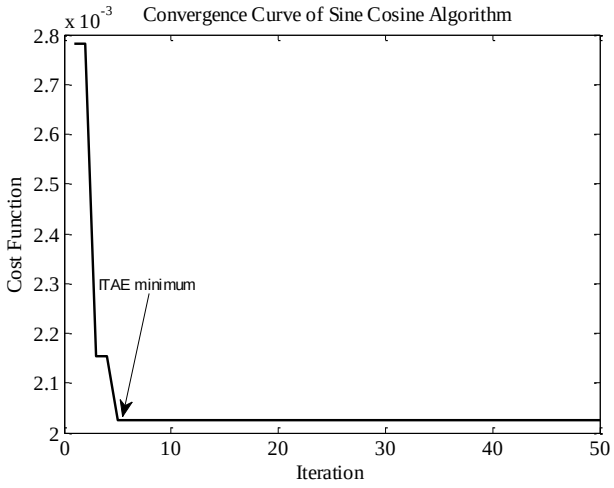

Figure. 5 Convergence of SCA

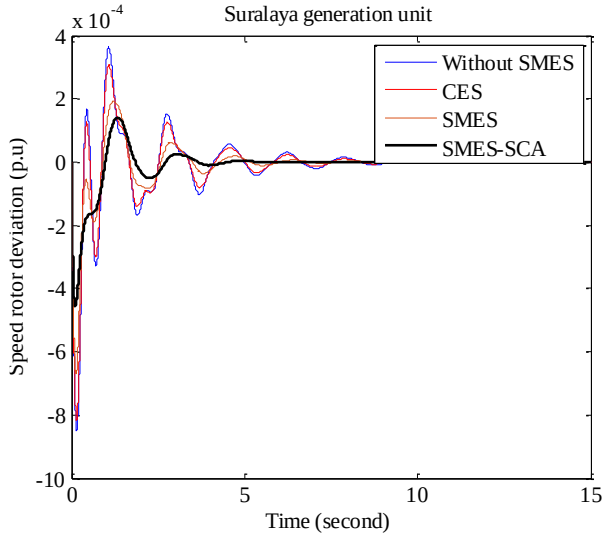

Figure. 6 Rotor speed response

Table 1. Overshoot value of all power plant

Unit	Overshoot			
	Without SMES	CES	SMES	SMES-SCA
Suralaya	-0.000843	-0.000809	-0.000660	-0.000448
Muara Tawar	-0.000464	-0.000447	-0.000357	-0.000249
Cirata	-0.000423	-0.000400	-0.000334	-0.000253
Saguling	-0.000365	-0.000347	-0.000282	-0.000209
Tanjung Jati	-0.000415	-0.000393	-0.000326	-0.000243
Gresik	-0.000381	-0.000367	-0.000307	-0.000242
Paiton	-0.000414	-0.000399	-0.000335	-0.000268
Grati	-0.000389	-0.000369	-0.000300	-0.000220

4. Results and discussions

In this paper third case studies are considered to investigate the dynamic performance of Jawa Indonesia power grid with SMES based on the SCA.

Table 2. Settling time value of all power plant

Unit	Setling Time			
	Without SMES	CES	SMES	SMES-SCA
Suralaya	10.97	10.84	6.63	5.51
Muara Tawar	11.54	10.88	7.40	6.01
Cirata	11.58	10.76	7.57	6.28
Saguling	11.59	10.97	7.68	6.43
Tanjung Jati	11.63	11.06	7.61	5.82
Gresik	11.68	11.02	7.63	5.59
Paiton	11.65	10.89	7.55	6.23
Grati	14.23	14.04	7.77	6.91

The first case study focused on how the performance react to static disturbances. While the second case study focused on how the proposed control method handle the variation of the load. The last case study is compared the proposed results with the existing method. To thoroughly investigate the efficacy of the proposed method, different scenarios are considered for case studies one and two. The first scenario is system without SMES. The second scenario is system with CES. The third scenario is system with SMES, and the last scenario is our proposed method.

4.1 Case study 1

This case study focused on investigating the dynamics response of rotor speed of the Jawa Indonesia power grid. To investigate the dynamics performance of the rotor speed, small perturbation is given in the Suralaya bus load. The small perturbation is 0.1 step input of load changing. Fig. 7 shows the dynamic response of rotor speed in Suralaya power plant. The blue line indicated the base condition of Jawa Indonesia power grid (without SMES). Jawa Indonesia power grid with capacitor energy storage is presented with the red line. In addition, the Jawa Indonesia power grid with SMES is indicated with brown line. Moreover, the black line indicates the Jawa Indonesia power grid with the proposed controller method (SMES based on SCA). From Fig. 6, it is noticeable that the proposed method not only help the power plant in the first swings, but also help the power plant to find the steady state condition. This is indicated by the smallest overshoot and fastest settling time of the system with the proposed method. SMES could provide damping when there is disturbance. SMES provide damping in the system by transferring electrical power to the load. Hence, the balance between mechanical power and electrical power can be accelerated. In addition, the difference between mechanical power and electrical power is not too big as some of the

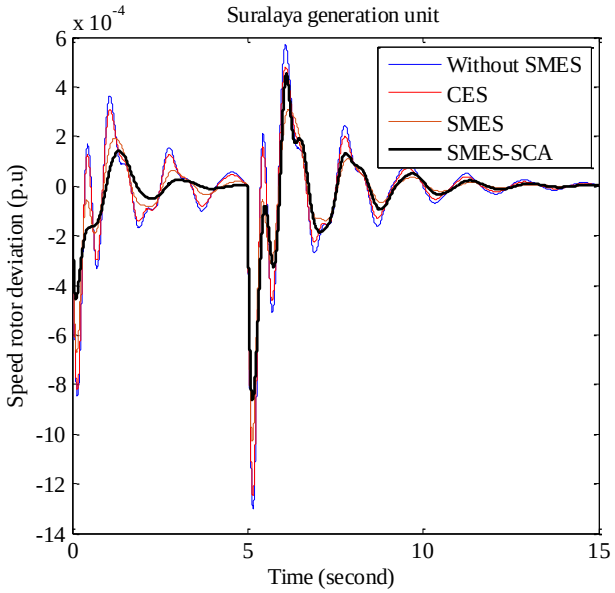

Figure. 7 Rotor speed dynamics response

Table 3. Overshoot value of all power plant under load variation

Unit	Overshoot			
	Without SMES	CES	SMES	SMES-SCA
Suralaya	-0.00129	-0.00124	-0.00101	-0.00084
Muara Tawar	-0.00073	-0.00069	-0.00056	-0.00049
Cirata	-0.00069	-0.00064	-0.00053	-0.00049
Saguling	-0.00058	-0.00055	-0.00045	-0.00043
Tanjung Jati	-0.00065	-0.00062	-0.000518	-0.000489
Gresik	-0.00061	-0.00058	-0.000489	-0.000468
Paiton	-0.00066	-0.00063	-0.000534	-0.000511
Grati	-0.00062	-0.00059	-0.000476	-0.000448

Table 4. Settling time value of all power plant under load variation

Generation Unit	Setling Time			
	Without SMES	CES	SMES	SMES-SCA
Suralaya	14.50	14.15	13.33	12.57
Muara Tawar	14.92	14.83	13.50	13.27
Cirata	14.98	14.78	13.42	13.10
Saguling	14.89	14.65	13.45	13.21
Tanjung Jati	14.91	14.85	13.23	13.15
Gresik	14.87	14.75	13.38	13.18
Paiton	14.95	14.92	13.25	13.10
Grati	14.97	14.82	13.28	13.25

Table 5. Overshoot value of suralaya power plant under different optimization method

Unit	Overshoot			
	GA	PSO	FA	Proposed Method
Suralaya	-0.0007	-0.00062	-0.00055	-0.000448

electrical power is supplied by SMES.

Table 1 and 2 shows the overshoot and settling time of all the power plant rotor speed dynamic response. It is noticeable that by adding the proposed controller method in Suralaya power plant make all the power plant have positive effect. It is observed that, all the power plant has the smallest overshoot and the fastest settling time compared to the other scenario in this paper. Although the overshoot value is small but when the higher disturbance emerges the possibility of the system experience out of synchronization is high. In addition, system with proposed method experience longer settling time that can also lead to unsynchronized conditions.

4.2 Case study 2

In the second case study, the proposed method is tested against load variation. The first load changing is emerged at 0 second while the second perturbation emerges at 5 second. The first load changing value is 0.1 pu (100 MW) and the second load changing value is 0.15 pu (150 MW). Fig. 7 shows the dynamic response of rotor speed Suralaya power plant. It is noticeable that for booth load changing the Suralaya power plant with the proposed method still has the best rotor speed dynamic response compared to the other scenarios.

Tables 3 and 4 show the overshoot and settling time of rotor speed of all power plant. It is noticeable that in all power plant, system with proposed controller method is superior compared to other scenarios. It is indicated by the small overshoot and fastest settling time.

4.3 Case study 3

In the third case study, the overshoot comparison between proposed method and existing method is carried out. The other algorithms are used is FA, genetic algorithm (GA) and PSO [12]. Table 5 shows the overshoot comparison between the proposed method and the existing method. It is noticeable that the proposed method shows less overshoot compared to the PSO, GA and FA [13].

5. Conclusions

This paper proposed a method to add power oscillation damping using SMES. To get a better performance, SCA is used as optimization method for designing SMES parameter. Jawa Indonesia power grid is used as the test system of this paper. From the simulation results, it is noticeable that the proposed method can be used to emulate power oscillation damping to the system. This is indicated by the

smallest overshoot and the fastest settling time (Overshoot and settling time of Suralaya power plant -0.000448 and 5.51 second). Furthermore, for further research additional inertia controller can be added to SMES to get a better oscillation damping.

Appendix

Table 6. List of notations used in this paper

Symbol	Meaning
T_{dc}	Time delay of the converter
I_d	Current in the inductor
E_d	DC voltage applied in inductor
k_0	Gain constant
L	Inductor coil
k_{id}	Feedback gain
T_m	Turbine mechanical torque
T_e	Rotor electrical torque
T_a	Torque acceleration
δ_m	Electromechanical torque
J	Total moment inertia
P_m	Rotor mechanical power
P_e	Rotor electrical power
P_a	Acceleration power
ω_m	Rotor speed
ω_s	Rotor speed
p	Poles
δ	Rotor angle
X_d	d-axis synchronous reactance
X_d'	Transient reactance
X_d''	Sub transient reactance
X_q	q-axis synchronous reactance
X_q'	q-axis transient reactance
X_q''	q-axis sub transient reactance

Conflicts of interest

The authors declare no conflict of interest.

Author contributions

Conceptualization, Muhammad Abdillah, Imam Wahyudi Farid and Herlambang Setiadi; methodology, Muhammad Abdillah, IBG Manuaba and Agileswari K. Ramasamy; Muhammad Abdillah, Herlambang Setiadi and Renuga Verayiah; validation, Muhammad Abdillah and Herlambang Setiadi; formal analysis, and Agileswari K. Ramasamy; investigation, Muhammad Abdillah and Renuga Verayiah; resources, Muhammad Abdillah; writing original draft preparation, Muhammad Abdillah; writing review and editing,, Maryati Binti Marsadek, IBG Manuaba and Herlambang Setiadi; visualization, Muhammad Abdillah, Renuga Verayiah, All authors have read and agreed to the published version of the manuscript.

References

[1] P. Kundur, J. Paserba, V. Ajjarapu, G. Anderson, A. Bose, C. Canizares, N. Hatziargyriou, D. Hill, A. Stankovic, C. Taylor, T. Van Cutsem, and V. Vittal, "Definition and classification of power system stability IEEE/CIGRE joint task force on stability terms and definitions", *IEEE Transactions on Power Systems*, Vol. 19, No. 3, pp. 1387–1401, 2004.

[2] U. Markovic, O. Stanojev, P. Aristidou, E. Vrettos, D. S. Callaway, and G. Hug, "Understanding small-signal stability of low-inertia systems", *IEEE Transactions on Power Systems*, Vol. 36, No.5, pp. 3997-4017, 2021.

[3] T. Kerdphol, F. S. Rahman, M. Watanabe, and Y. Mitani, "Virtual Inertia Synthesis and Control", In: *Proc. of 1st ed. Cham: Springer International Publishing*, 2021, doi: 10.1007/978-3-030-57961-6.

[4] S. Dhundhara and Y. P. Verma, "Capacitive energy storage with optimized controller for frequency regulation in realistic multisource deregulated power system", *Energy*, Vol. 147, pp. 1108–1128, 2018, doi: https://doi.org/10.1016/j.energy.2018.01.076.

[5] K. Singh, "Enhancement of frequency regulation in tidal turbine power plant using virtual inertia from capacitive energy storage system", *Journal of Energy Storage*, Vol. 35, p. 102332, 2021.

[6] H. Setiadi, N. Mithulananthan, R. Shah, M. R. Islam, A. Fekih, A. U. Krismanto, and M. Abdillah, "Multi-Mode Damping Control Approach for the Optimal Resilience of Renewable-Rich Power Systems", *Energies (Basel)*, Vol. 15, No. 9, p. 2972, 2022.

[7] M. Ramírez, R. Castellanos, G. Calderón, and O. Malik, "Placement and sizing of battery energy storage for primary frequency control in an isolated section of the Mexican power system", *Electric Power Systems Research*, Vol. 160, pp. 142–150, 2018, doi: https://doi.org/10.1016/j.epsr.2018.02.013.

[8] I. A. Chidambaram and B. Paramasivam, "Control performance standards based load-frequency controller considering redox flow batteries coordinate with interline power flow controller", *Journal of Power Sources*, Vol. 219, pp. 292–304, Dec. 2012, doi: http://dx.doi.org/10.1016/j.jpowsour.2012.06.048.

[9] S. Oshnoei, A. Oshnoei, A. Mosallanejad, and F. Haghjoo, "Novel load frequency control scheme for an interconnected two-area power system including wind turbine generation and redox flow battery", *International Journal of Electrical Power & Energy Systems*, Vol. 130, p. 107033, 2021.

[10] M. G. Molina and P. E. Mercado, "Power Flow Stabilization and Control of Microgrid with Wind Generation by Superconducting Magnetic Energy Storage", *IEEE Transactions on Power Electronics*, Vol. 26, No. 3. pp. 910–922, 2011, doi: 10.1109/TPEL.2010.2097609.

[11] M. M. T. Ansari and S. Velusami, "Dual mode linguistic hedge fuzzy logic controller for an isolated wind–diesel hybrid power system with superconducting magnetic energy storage unit", *Energy Conversion and Management*, Vol. 51, No. 1, pp. 169–181, 2010.

[12] H. K. Abdulkhader, J. Jacob, and A. T. Mathew, "Fractional-order lead-lag compensator-based multi-band power system stabiliser design using a hybrid dynamic GA-PSO algorithm", *IET Generation, Transmission & Distribution*, Vol. 12, No. 13, pp. 3248–3260, 2018, doi: 10.1049/iet-gtd.2017.1087.

[13] M. Singh, R. N. Patel, and D. D. Neema, "Robust tuning of excitation controller for stability enhancement using multi-objective metaheuristic Firefly algorithm," *Swarm and Evolutionary Computation*, Vol. 44, pp. 136–147, 2019, doi: 10.1016/j.swevo.2018.01.010.

[14] M. R. Shakarami and I. F. Davoudkhani, "Wide-area power system stabilizer design based on Grey Wolf Optimization algorithm considering the time delay", *Electric Power Systems Research*, Vol. 133, pp. 149–159, 2016, doi: 10.1016/j.epsr.2015.12.019.

[15] S. Gurung, F. Jurado, S. Naetiladdanon, and A. Sangswang, "Comparative analysis of probabilistic and deterministic approach to tune the power system stabilizers using the directional bat algorithm to improve system small-signal stability", *Electric Power Systems Research*, Vol. 181, p. 106176, 2020.

[16] L. Khrissi, N. E. Akkad, H. Satori, and K. Satori, "Clustering method and sine cosine algorithm for image segmentation", *Evolutionary Intelligence*, Vol. 15, No. 1, pp. 669–682, 2022, doi: 10.1007/s12065-020-00544-z.

[17] S. Mirjalili, "SCA: A Sine Cosine Algorithm for solving optimization problems", *Knowledge-Based Systems*, Vol. 96, pp. 120–133, 2016, doi: 10.1016/j.knosys.2015.12.022.

[18] T. Kerdphol, M. Watanabe, K. Hongesombut, and Y. Mitani, "Self-adaptive virtual inertia control-based fuzzy logic to improve frequency stability of microgrid with high renewable penetration", *IEEE Access*, Vol. 7, pp. 76071–76083, 2019.

[19] T. Kerdphol, F. S. Rahman, M. Watanabe, and Y. Mitani, "Robust virtual inertia control of a low inertia microgrid considering frequency measurement effects", *IEEE Access*, Vol. 7, pp. 57550–57560, 2019.

[20] T. Kerdphol, F. S. Rahman, Y. Mitani, M. Watanabe, and S. K. Küfeoğlu, "Robust virtual inertia control of an islanded microgrid considering high penetration of renewable energy", *IEEE Access*, Vol. 6, pp. 625–636, 2017.

[21] H. Setiadi, A. Swandaru, D. A. Asfani, T. H. Nasution, M. Abdillah, and A. U. Krismanto, "Coordinated Design of DIPSS and CES Using MDEA for Stability Enhancement: Jawa-Bali Indonesian Power Grid Study Case", *International Journal of Intelligent Engineering and Systems*, Vol. 15, No. 1, pp. 251–261, 2022, doi: 10.22266/ijies2022.0228.23.

[22] V. Vittal, J. D. McCalley, P. M. Anderson, and A. A. Fouad, "Power system control and stability", *John Wiley & Sons*, 2019.

[23] H. Setiadi, N. Mithulananthan, R. Shah, T. Raghunathan, and T. Jayabarathi, "Enabling resilient wide-area POD at BESS in Java, Indonesia 500 kV power grid", *IET Generation, Transmission & Distribution*, Vol. 13, No. 16, pp. 3734–3744, 2019.

[24] L. Abualigah and A. Diabat, "Advances in sine cosine algorithm: a comprehensive survey", *Artificial Intelligence Review*, pp. 1–42, 2021.

[25] S. Gupta and K. Deep, "Improved sine cosine algorithm with crossover scheme for global optimization", *Knowledge-Based Systems*, Vol. 165, pp. 374–406, 2019.

[26] S. Gupta, K. Deep, S. Mirjalili, and J. H. Kim, "A modified sine cosine algorithm with novel transition parameter and mutation operator for global optimization", *Expert Systems with Applications*, Vol. 154, p. 113395, 2020.